



New VVV Survey Globular Cluster Candidates in the Milky Way Bulge*

Dante Minniti^{1,2,3}, Douglas Geisler⁴, Javier Alonso-García^{2,5}, Tali Palma⁶, Juan Carlos Beamín^{2,7}, Jura Borissova^{2,7}, Marcio Catelan^{2,4}, Juan J. Clariá⁶, Roger E. Cohen⁸, Rodrigo Contreras Ramos^{2,9}, Bruno Dias¹⁰, Jose G. Fernández-Trincado^{4,11}, Matías Gómez¹, Maren Hempel⁹, Valentin D. Ivanov¹², Radostin Kurtev^{2,7}, Phillip W. Lucas¹³, Christian Moni-Bidin¹⁴, Joyce Pullen², Sebastian Ramírez Alegría¹⁴, Roberto K. Saito¹⁵, and Elena Valenti¹²

¹Departamento de Física, Facultad de Ciencias Exactas, Universidad Andrés Bello, Av. Fernández Concha 700, Las Condes, Santiago, Chile

²Instituto Milenio de Astrofísica, Santiago, Chile

³Vatican Observatory, V00120 Vatican City State, Italy

⁴Departamento de Astronomía, Casilla 160-C, Universidad de Concepción, Casilla 160-C, Concepción, Chile

⁵Unidad de Astronomía, Facultad Cs. Básicas, Universidad de Antofagasta, Avda. U. de Antofagasta 02800, Antofagasta, Chile

⁶Observatorio Astronómico, Universidad Nacional de Córdoba, Laprida 854, Córdoba, Argentina

⁷Instituto de Física y Astronomía, Universidad de Valparaíso, Av. Gran Bretaña 1111, Playa Ancha, Casilla 5030, Valparaíso, Chile

⁸Space Telescope Science Institute, 2700 San Martin Drive, Baltimore, USA

⁹Pontificia Universidad Católica de Chile, Instituto de Astrofísica, Av. Vicuña Mackenna 4860, Santiago, Chile

¹⁰European Southern Observatory, Alonso de Cordova 3107, Vitacura, Santiago, Chile

¹¹Institut Utinam, CNRS UMR6213, Univ. Bourgogne Franche-Comté, OSU THETA, Observatoire de Besançon, BP 1615, 25010 Besançon Cedex, France

¹²European Southern Observatory, Karl-Schwarzschild-Str. 2, D-85748 Garching bei München, Germany

¹³Dept. of Astronomy, University of Hertfordshire, Hertfordshire, UK

¹⁴Instituto de Astronomía, Universidad Católica del Norte, Antofagasta, Chile

¹⁵Departamento de Física, Universidade Federal de Santa Catarina, Trindade 88040-900, Florianópolis, SC, Brazil

Received 2017 September 14; revised 2017 October 19; accepted 2017 October 23; published 2017 November 3

Abstract

It is likely that a number of Galactic globular clusters remain to be discovered, especially toward the Galactic bulge. High stellar density combined with high and differential interstellar reddening are the two major problems for finding globular clusters located toward the bulge. We use the deep near-IR photometry of the VISTA Variables in the Vía Láctea (VVV) Survey to search for globular clusters projected toward the Galactic bulge, and hereby report the discovery of 22 new candidate globular clusters. These objects, detected as high density regions in our maps of bulge red giants, are confirmed as globular cluster candidates by their color–magnitude diagrams. We provide their coordinates as well as their near-IR color–magnitude diagrams, from which some basic parameters are derived, such as reddenings and heliocentric distances. The color–magnitude diagrams reveal well defined red giant branches in all cases, often including a prominent red clump. The new globular cluster candidates exhibit a variety of extinctions ($0.06 < A_{K_s} < 2.77$) and distances ($5.3 < D < 9.5$ kpc). We also classify the globular cluster candidates into 10 metal-poor and 12 metal-rich clusters, based on the comparison of their color–magnitude diagrams with those of known globular clusters also observed by the VVV Survey. Finally, we argue that the census for Galactic globular clusters still remains incomplete, and that many more candidate globular clusters (particularly the low luminosity ones) await to be found and studied in detail in the central regions of the Milky Way.

Key words: Galaxy: bulge – Galaxy: general – globular clusters: general

1. Introduction

Globular clusters (GCs) are among the best tools to study the formation and evolution of galaxies, including the Milky Way. Our Galaxy is slightly less massive than the Andromeda galaxy, which hosts a large globular cluster system with more than 600 members (Barmby & Huchra 2001; Huxor et al. 2014). Yet, the total number of known Galactic globular clusters is surprisingly small in comparison to that of Andromeda. The 2010 December compilation of the Harris (1996) catalog lists 157 GCs in the Milky Way. As far as we know, 22 more objects have recently been discovered, namely, Kopusov 1 (Kopusov et al. 2007), Segue 3 (Belokurov et al. 2010), SDSSJ1257+3419 (Sakamoto & Hasegawa 2006), AL3 (Ortolani et al. 2006), FSR 584 (Bica et al. 2007), FSR 1767 (Bonatto et al. 2007), FSR 190 (Froeblich et al. 2008), Pfliederer 2 (Ortolani et al. 2009), VVV CL001 (Minniti

et al. 2011), Mercer 5 (Longmore et al. 2011), VVV CL 002 and VVV CL 003 (Moni Bidin et al. 2011), Muñoz 1 (Muñoz et al. 2012), Balbinot 1 (Balbinot et al. 2013), Laevens 1 = Crater (Belokurov et al. 2014; Laevens et al. 2014), VVV CL 119, VVV CL 143, and VVV CL 150 (Borissova et al. 2014), Kim 1 (Kim & Jerjen 2015), Kim 2 (Kim et al. 2015), Kim 3 (Kim et al. 2016), and FSR 1716 = VVV-GC05 (Minniti et al. 2017). The GC nature of some of these objects remains to be confirmed (Borissova et al. 2014), especially in the case of very low luminosity clusters. In any case, if all of them are genuine GCs, this would bring the total Milky Way sample to $N = 179$ GCs. Consequently, in spite of the recent discoveries, the Milky Way GC system appears to be substantially smaller than that of the Andromeda galaxy. Harris et al. (2013) find that the specific frequency (number of GCs per unit galaxy luminosity) of the Andromeda GC system is 1.8 times higher than that of the Galaxy. This implies either that the Galaxy has been relatively inefficient at making GCs, or that we have been inefficient in finding them. The former is unlikely given the nearly universal GC formation efficiency

* Based on observations taken within the ESO programs 179.B-2002 and 298.D-5048.

(Harris et al. 2013). Thus, we are left with the second alternative.

The addition of several new low luminosity globular clusters would add to the total number of GCs in the MW, but it would not affect the general properties of the GC system used to study other galaxies. For example, it would not significantly affect the total luminosity (or total stellar mass) of the MW GC system. Likewise, regarding the study of distant extragalactic GCS, the present candidates would not be relevant since they would remain beyond detection in distant galaxies. However, it is necessary to have a complete census of MW GCs, because our Galaxy is the only major galaxy that can be studied in detail down to the faintest members. These objects are interesting for a variety of reasons. Low luminosity GCs are important for the study of the dynamical evolution of the GCS of the MW, as they would be survivors that trace the relative importance of different disruption processes, like dynamical friction, disk and bulge shocking, evaporation, etc. (e.g., Weinberg 1994). The presence of low luminosity objects is also relevant in the context of galaxy formation models, where there is a continuous build up of the spheroidal component by accretion of small proto-galactic fragments (e.g., Helmi & White 1999). In this context, Tissera et al. (2017) studied the survival of structures in the inner regions of the MW, finding that some remnants may be detected even within the bulge, and the old GCs may be representative (or tracers) of these fragments, and have been useful in studying the formation and evolution of the Galaxy.

How many GCs are missing in current Milky Way catalogs, and how can we find them? While most of the recent GC discoveries have been made in the Galactic halo thanks to recent imaging surveys like the Sloan Digital Sky Survey (York et al. 2000), another obvious place to look for missing GCs is toward the Galactic bulge, which hosts both metal-poor and metal-rich GCs. The metal-rich GCs with small Galactocentric distances are associated with the Milky Way bulge (Minniti 1995; Barbuy et al. 1998). For example, in the hierarchical formation scenario for the Galactic spheroid, Cote et al. (2000) identified the bulge as the dominant proto-galactic building block, and these metal-rich GCs would belong to its associated GC system.

Some GCs may remain camouflaged toward low Galactic latitudes because of high extinction and/or stellar crowding, (e.g., Minniti 1995; Barbuy et al. 1998; Ivanov et al. 2005, 2017). One of the goals of the VISTA Variables in the Vía Láctea (VVV) Survey was to search for such GCs, and measure their astrophysical parameters in the near-IR (Minniti et al. 2010). Indeed, our previous VVV GC searches identified a few new Galactic GCs (Minniti et al. 2011; Moni Bidin et al. 2011; Borissova et al. 2014; Minniti et al. 2017). However, the VVV Survey data could reveal many more such objects disguised in the central regions of the Milky Way, as current attempts at uncovering them have not been exhaustive. In this paper, we present a new way of searching for these objects, using selected cuts in the Wesenheit Ks-band magnitude W_K versus $J - K_s$ color-magnitude diagram (CMD) in order to create maps of bulge red giants and search for good GC candidates, for which we present deep near-IR CMDs to further investigate their GC nature. As described below, here we have found 22 new candidate Galactic GCs, that would bring the total population in the Milky Way up to almost 200 members.

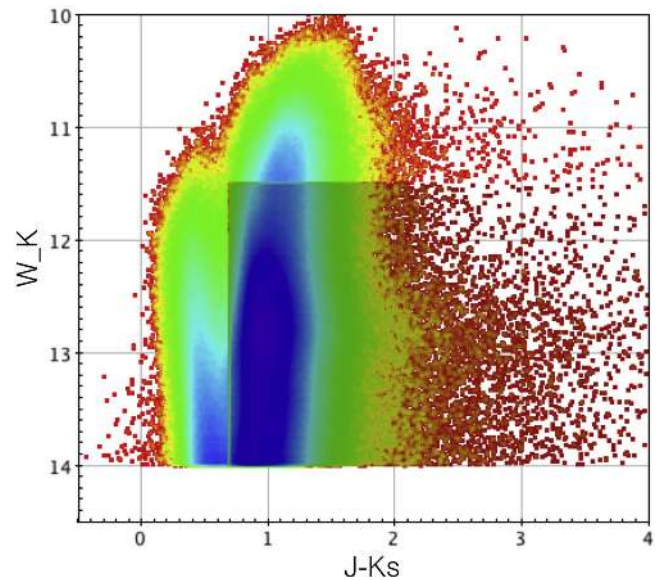


Figure 1. CMD of the region within $-10.0 \text{ deg} < l < 10.5 \text{ deg}$, and $-8 \text{ deg} < b < -6.75 \text{ deg}$ (corresponding to VVV tiles b229 to b242) using Wesenheit magnitudes $W_K = K_s - 0.45 * (J - K_s)$. The cuts made in order to select distant red giants are shown.

2. Selection of Globular Cluster Candidates

We use data from the VVV Survey (Minniti et al. 2010; Saito et al. 2012) acquired with the VIRCAM camera at the VISTA 4 m telescope at the ESO Paranal Observatory (Emerson & Sutherland 2010) between years 2010 and 2016, and reduced at the Cambridge Astronomical Survey Unit (CASU) with the VIRCAM pipeline v1.3. The PSF photometry used to make the deep near-IR CMDs was done with DoPhot following Alonso-García et al. (2015).

In order to minimize the reddening problem, we have used the Wesenheit magnitudes (see, e.g., Majaess et al. 2011; Bhardwaj et al. 2016) defined here as $W_K = K_s - 0.45 * (J - K_s)$. Selected cuts in the W_K versus $J - K_s$ CMD allow us to eliminate most of the background disk stars, retaining distant red giants (Figure 1). We adopted a slope for the reddening vector of 0.45 that fits the behavior of the red clump in our near-IR bulge CMDs. The actual value of the slope of the reddening vector is inconsequential for the density maps, as confirmed by using different slopes ranging from 0.428 from Alonso-García et al. (2015) to 0.72 from Cardelli et al. (1989). Limiting the magnitude range to $11.5 < W_K < 14$ enabled us to eliminate saturated objects, as well as unreddened local dwarfs and reddened foreground disk stars that mix with the more distant red subgiant branch stars. The cut made in color (usually $J - K_s > 0.7 \text{ mag}$) made it possible for us to eliminate the less reddened foreground disk stars that are bluer than the bulge red giant branch (RGB). We do not apply any cuts to the reddest stars, in order not to miss significantly reddened GCs.

We then built density maps using only the selected red giants, and identified the apparent overdensities to mark the location of GC candidates. The identification of the overdensities was done by visual inspection by one of us (D.M.). The whole bulge was examined, excluding only the Galactic plane region (mostly $-1 \text{ deg} < b < 1 \text{ deg}$), where extinction and crowding are more pronounced (Figure 2). Initially, we identified more than 200 overdensities that are apparently consistent with the expected sizes of known Galactic GCs

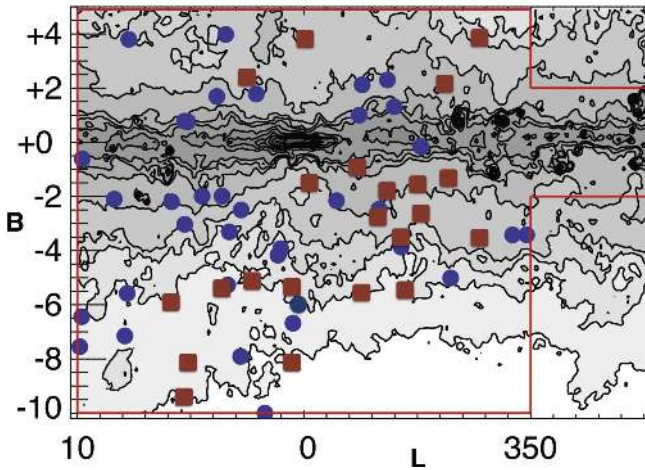


Figure 2. Map of the Galactic bulge region oriented along Galactic coordinates l, b . This map shows the location of previously known GCs (blue circles) and the newly discovered ones (red squares), overlaid on the extinction contours of Schlafly & Finkbeiner (2011). The red line encloses the whole bulge region mapped by the VVV survey. The apparent black dots are not globular clusters but cores of dense clouds.

located at the bulge distance ($\sim 2\text{--}5$ arcmin). Upon closer inspection of the VVV Survey images looking for overdensities of fainter stars, and inspection of the CMDs looking for well defined RGBs (and red clumps in some cases), most of them appeared to be just random groupings of red giants. Importantly, this search showed that all but one (BH261) of the known GCs present in the region were included in our list (this was a blind search in the sense that we did not input their coordinates a priori). After discarding these known GCs, we selected only the 34 best cluster candidates (with the highest overdensities). As a final step, we visually compared the CMDs of the GC candidates with those of the known bulge GCs observed by the VVV Survey. This allowed us to select a final sample containing the 22 best remaining GC candidates studied here. The RGB for each of the final candidates does not look like that of an open cluster, with well populated sequences. The remaining dozen candidates can be either chance asterisms, open star clusters, or GCs badly affected by field contamination and differential reddening.

As part of the final selection, we also compared the CMDs centered on the cluster candidates with their respective background fields, in order to verify that the cluster RGB (and its associated red clump) appears tighter than that observed in the background. These background fields were selected as similar areas located 5 arcmin away from the measured cluster centers. Interestingly, most of the new GC candidates are hidden in plain sight, concealed in an ocean of field stars. Only one of the new globular candidates (cluster 14 in Table 1) is actually cloaked behind regions of large extinction. However, we have so far avoided the regions with highest extinction near the Galactic plane (mostly within $-1 < b < 1$ deg), so in effect there is still a “zone of avoidance” which could easily harbor a number of additional GCs.

After the selection was made, we used the statistical decontamination procedure described by Palma et al. (2016) and Minniti et al. (2017), in order to better discriminate the observed cluster CMDs (shown in the leftmost panels of Figure 3) from their respective background fields. In summary, this process consists in selecting four circular background fields per cluster, of the same area but centered about 5 arcmin away

from its center (Figure 3, central panels). We then subtracted from the cluster CMD the stars that fall in the same intervals of color and magnitude of the background CMDs, as shown in the rightmost panels of Figure 3.

We also measured the mean cluster reddening values based on the observed RGBs or on the red clump colors. In order to obtain these reddenings, we adopted a red clump mean intrinsic color $(J - K_s)_0 = 0.61 \pm 0.01$, following Alves et al. (2002), Grocholski & Sarajedini (2002), and Minniti et al. (2011). The observed mean red clump colors are listed in Table 1, yielding the reddenings also listed in this table. In general, these reddening values are in excellent agreement with the extinction determinations of Schlafly & Finkbeiner (2011), and Gonzalez et al. (2012).

Table 1 presents in succession the GC identification number, the Equatorial coordinates, the Galactic (l, b) coordinates, the mean K_s -band magnitude and $J - K_s$ color of the horizontal branch, the comparison clusters, the differences in magnitudes and colors with the comparison GCs, the distances and reddenings measured as described below, and a preliminary metallicity classification.

3. Near-IR Color–Magnitude Diagrams

Figure 3 shows the CMDs for the new candidate GCs, along with a couple of comparison clusters (NGC6642 and NGC6637). The CMDs centered on the new GC candidates reveal a populated cluster RGB that is tighter than that of their respective comparison regions. This ensures that the object is most likely a real GC, as opposed to a window in the dust distribution toward the bulge, which should exhibit a wider RGB, typical of the Galactic bulge population.

For half of the clusters, we clearly see a well defined red clump in the cluster RGB, which is more compact than the bulge field red clump. The field shows a wider spread in magnitudes and colors because of the line-of-sight depth and wide range of stellar metallicities. Therefore, we classified these objects as metal-rich GCs. For these objects, we used the comparison GCs with $[\text{Fe}/\text{H}] > -1$. On the other hand, the other half of the clusters that do not show a prominent red clump but appear to have a well defined RGB, are classified as metal-poor. For these objects, we used the comparison GCs with $[\text{Fe}/\text{H}] > -1$. These classifications listed in the last column of Table 1 should be considered preliminary, until follow-up spectroscopic metallicities are available.

The fiducial RGBs for GCs in the K_s versus $J - K_s$ plane can be used to measure their metallicities (e.g., Ivanov & Borissova 2002; Valenti et al. 2004; Cohen et al. 2017). However, this method is risky to apply for all the low luminosity clusters found here, which have few red giants, in the presence of a heavily contaminating field with numerous bulge giants and also, in many cases, with the existence of differential reddening. Proper motions are clearly needed in order to better clean up the RGBs of the cluster candidates. Following the same criteria, it is very difficult to measure the total luminosities of the new candidate GCs. In fact, most of the new GCs cannot be directly seen in the VVV images, revealing that the new GCs have lower luminosity than the previously known GCs in the region. We are currently looking at ways of measuring their radial profiles in the presence of the overwhelming stellar background to be able to estimate the total luminosities and structural parameters.

Table 1
New Globular Cluster Candidates Discovered Using Near-IR VVV Survey Photometry^a

ID	R.A. 2000	Decl. 2000	long.	lat.	K_{SHB}	$J - K_{\text{SHB}}$	Comp.	ΔK_s	$\Delta (J - K_s)$	D(kpc)	$E(J - K_s)$	Class
01	278.698	-28.711	5.370	-9.347	13.10	0.75	N6642	0.00	0.01	8.1	0.14	mp
02	277.510	-28.440	5.151	-8.291	12.90	0.76	N6522	-0.30	0.01	6.6	0.15	mp
03	275.097	-32.408	0.624	-8.215	12.80	0.73	N6642	-0.30	0.03	7.0	0.12	mp
04	273.896	-28.300	3.812	-5.398	12.70	0.80	N6624	-0.40	0.10	5.3	0.19	mr
05	269.273	-35.690	355.445	-5.501	13.25	0.83	N6642	0.15	0.07	8.5	0.22	mp
06	272.092	-31.105	0.585	-5.348	13.20	0.82	N6642	0.10	0.06	8.4	0.21	mp
07	270.398	-33.918	357.418	-5.456	13.40	0.82	N6624	0.10	0.18	6.8	0.21	mr
08	275.581	-26.628	5.998	-5.945	12.90	0.84	N6642	-0.20	0.08	7.2	0.23	mp
09	257.624	-33.251	352.236	3.859	13.50	0.93	N6522	0.30	0.18	8.5	0.32	mp
10	265.693	-37.315	352.539	-3.870	13.80	1.05	N6522	0.60	0.30	9.5	0.44	mp
11	266.138	-34.723	354.942	-2.824	13.30	1.15	N6624	0.00	0.51	5.9	0.54	mr
12	265.650	-25.556	2.530	2.341	13.15	1.23	N6624	-0.10	0.55	5.6	0.62	mr
13	263.975	-34.989	353.774	-1.462	13.70	1.50	TER6	-0.10	0.05	6.2	0.99	mr
14	265.762	-31.120	357.847	-0.668	14.00	2.70	TER12	1.20	1.20	6.3	2.09	mr
15	266.053	-32.790	356.555	-1.754	13.45	1.70	N6637	0.05	1.10	7.0	1.09	mr
16	260.347	-32.821	353.912	2.248	13.90	1.57	N6637	0.00	0.95	7.0	1.06	mr
17	272.905	-29.538	2.304	-5.218	12.70	0.79	N6637	-0.70	0.19	6.0	0.18	mr
18	262.716	-27.276	359.665	3.637	13.50	1.25	N6637	0.10	0.65	7.9	0.64	mr
19	265.129	-33.962	355.152	-1.715	13.55	1.23	N6637	0.15	0.63	8.1	0.62	mr
20	267.763	-29.842	359.835	-1.481	13.40	1.38	N6637	0.00	0.78	7.3	0.77	mr
21	267.670	-34.240	356.008	-3.657	13.10	1.03	N6642	0.00	0.28	7.6	0.42	mp
22	267.214	-33.062	356.828	-2.729	13.30	1.20	N6642	-0.20	0.44	6.6	0.59	mp

Note.

^a Typical photometric errors are $\sigma_{K_s} = 0.01$ mag, and $\sigma_{J,H} = 0.03$ mag; $\sigma_{K_{\text{SHB}}} = 0.10$; $\sigma_{J - K_{\text{SHB}}} = 0.03$; $\sigma_{\Delta K_s} = 0.05$; and $\sigma_{\Delta(J - K_s)} = 0.02$. Distances are accurate to ~ 1.5 kpc, and reddenings to $\sigma_{E(J - K_s)} = 0.05$.

We measured the heliocentric distances differentially with respect to selected comparison clusters also observed by the VVV Survey. We adopted the following distances for the comparison clusters from Harris (2010): $D_{\text{NGC6624}} = 6.8$ kpc; $D_{\text{NGC6522}} = 7.7$ kpc; $D_{\text{NGC6637}} = 8.8$ kpc; $D_{\text{NGC6642}} = 8.1$ kpc; $D_{\text{TER12}} = 4.8$ kpc; and $D_{\text{TER6}} = 6.8$ kpc. Our final distance estimates are listed in Table 1. Taking into account the uncertainties in the HB magnitudes ($\sigma_{K_{\text{HB}}} = 0.1$ mag), in the mean reddenings ($\sigma_{(J - K_s)} = 0.05$), and in the distances to the comparison clusters ($\sigma_D \approx 0.5$ kpc), we estimate an overall conservative distance error of $\sigma_D \approx 1.5$ kpc for the individual GC candidates.

If these are real GCs, they should be grouped more or less symmetrically around the Galactic center. As a consistency check, since most of the interstellar absorption should be foreground, the mean distance of all the globular cluster candidates should be near R_0 within the uncertainties ($R_0 = 8.3 \pm 0.2$ (statistical) ± 0.4 (systematic) kpc from the compilation of De Grijs & Bono 2017). The estimated mean distance of our candidates is 7.2 ± 0.3 kpc, which is close enough to the range of acceptable mean distances. Indeed, most of the GC candidates are located within the Galactic bulge physically, with distances between 6 and 9 kpc (Table 1), thus lying within 2–3 kpc of the Galactic center. The closest ones are clusters 04 and 12, located at $D = 5.3$ and 5.6 kpc, respectively, and classified as metal-rich GCs. According to the distances measured here, none of the new GC candidates are potential members of the Sgr dwarf galaxy, that is located behind the Galactic bulge at $D = 35$ kpc (Ibata et al. 1994). The most distant cluster of our sample is cluster 10, located at $D = 9.5$ kpc, and classified as a metal-poor GC.

4. Discussion

The present discoveries prompt many interesting questions: Are these low luminosity clusters younger or do they have different chemical compositions than the most luminous GCs? What can these objects tell us about the survival of structures deep into the Galactic potential well? What fractions of the GC population belong to the bulge, disk, or halo? How many GCs are still missing in the Milky Way?

There were 36 previously known GCs in the region mapped by the VVV Survey, and our candidates, if they are all genuine, augment the sample by more than 60%. This has only been possible thanks to the high quality near-IR images and photometry from the VVV Survey database. Considering that we have not thoroughly explored the Galactic plane and the outer bulge, we predict that the number of GCs in the region may be more than double the current estimate including the new candidates. Using the current technique, we expect that with the on-going extension of the VVV survey (VVVX) we might find about a dozen more good candidates. Considering also that halo surveys are finding low luminosity objects in recent years, we predict that the total number of GCs in the Milky Way may well be as high as 200 to 300 clusters. The present results forecast a bright future for the Large Synoptic Survey Telescope (LSST; Abell et al. 2009) as a powerful machine to discover low luminosity clusters throughout the whole Galaxy, although reddening will remain as a limiting factor.

These new objects can open the way for interesting further studies. For example, even though in many cases the CMDs show a hint of an old main sequence turn off at the faintest VVV magnitudes, accurate ages could be determined with deep CMDs from GeMS, *HST*, *JWST*, or WFIRST. It would also be

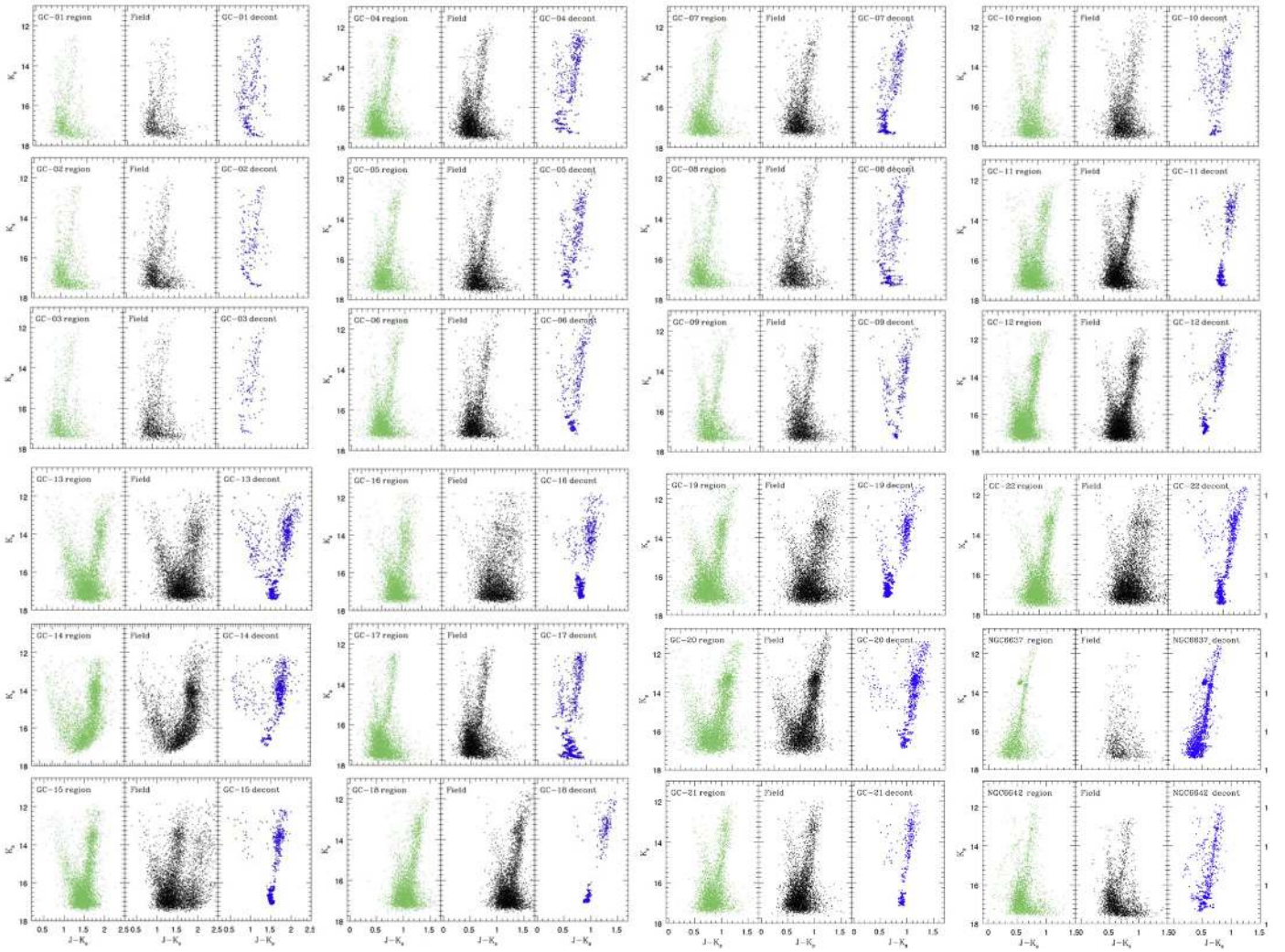


Figure 3. VVV PSF near-IR CMD for $R = 2$ arcmin fields centered on the sample GCs. We show for each cluster the observed CMDs (left panels in green), the equal-area background fields (middle panels in black), and the statistically decontaminated CMDs following the procedures of Palma et al. (2016)—right panels in blue. The last two objects show the CMDs for a couple of comparison GCs (NGC6637 and NGC6642), used as references for the distance measurements.

possible to measure metal abundances and radial velocities with APOGEE (Blanton et al. 2017) for the brightest candidates and with MUSE for the faintest ones (E. Valenti et al. 2017, in preparation). The velocities are needed in order to compute orbits after proper motion measurements are acquired. For some of the GC candidates, it may be possible to measure relative proper motions with the VVV data (Contreras Ramos et al. 2017). However, most of our GC candidates have red giants that are bright enough to have accurate absolute proper motion measurements with *Gaia* (E. Valenti et al. 2017, in preparation)

5. Conclusions






In summary, we have discovered 22 new GC candidates toward the central regions of the Milky Way thanks to two main reasons. First, the increase of the signal by filtering the background using the Wesenheit near-IR CMD allowed us to build density maps of distant red giants, wherein we could identify the known clusters and pick out new candidates. Second, the confirmation using deep PSF photometry from the VVV Survey allowed us to compare differentially the near-IR CMDs of the known GCs with the new GC candidates.

We provide the positions of the new GC candidates, measure their distances and reddenings, and classify 12 of them as metal-rich and 10 as metal-poor using the presence or absence of a prominent red clump, respectively, in the VVV near-IR CMDs. Most of the new GC candidates appear to be located physically within the Galactic bulge. An inspection of the VVV images reveals that the new GC candidates have lower luminosity than the previously known GCs in the region. This work also suggests that the Galactic GC census is still incomplete, especially in the low luminosity regime, and that the Milky Way may contain between 200 and 300 GCs in total.

We gratefully acknowledge data from the ESO Public Survey program ID 179.B-2002 taken with the VISTA telescope, and products from the Cambridge Astronomical Survey Unit (CASU). Support is provided by the BASAL Center for Astrophysics and Associated Technologies (CATA) through grant PFB-06, and the Ministry for the Economy, Development and Tourism, Programa Iniciativa Científica Milenio grant IC120009, awarded to the Millennium Institute of Astrophysics (MAS). D.M. and C.M.B. acknowledge support from FONDECYT Regular grants No. 1170121 and 1150060, respectively. S.R.A. was supported by the ESO-Government of

Chile Joint Committee. J.A.-G. acknowledges support by FONDECYT Iniciacion 11150916, and by the Ministry of Education through grant ANT-1656. R.K.S. acknowledges support from CNPq/Brazil through projects 308968/2016-6 and 421687/2016-9.

ORCID iDs

Dante Minniti  <https://orcid.org/0000-0002-7064-099X>
 Douglas Geisler  <https://orcid.org/0000-0002-3900-8208>
 Marcio Catelan  <https://orcid.org/0000-0001-6003-8877>
 Valentin D. Ivanov  <https://orcid.org/0000-0002-5963-1283>
 Phillip W. Lucas  <https://orcid.org/0000-0002-8872-4462>
 Roberto K. Saito  <https://orcid.org/0000-0001-6878-8648>
 Elena Valenti  <https://orcid.org/0000-0002-6092-7145>

References

- Abell, P. A., Allison, J., Anderson, S. F., et al. (The LSST Collaboration) 2009, arXiv:0912.0201
- Alonso-García, J., Dekany, I., Catelan, M., et al. 2015, *AJ*, 149, 99
- Alves, D., Rejkuba, M., Minniti, D., & Cook, K. 2002, *ApJL*, 573, L51
- Balbinot, E., Santiago, B. X., da Costa, L., et al. 2013, *ApJ*, 767, 101
- Barbuy, B., Bica, E., & Ortolani, S. 1998, *A&A*, 333, 117
- Barnby, P., & Huchra, J. P. 2001, *AJ*, 122, 2458
- Belokurov, V., Irwin, M. J., Koposov, S. E., et al. 2014, *MNRAS*, 441, 2124
- Belokurov, V., Walker, M. G., Evans, N. W., et al. 2010, *ApJL*, 712, L103
- Bhardwaj, A., Kanbur, S. M., Macri, L. M., et al. 2016, *AJ*, 151, 88
- Blanton, M. R., Bershady, M. A., Abolfathi, B., et al. 2017, *AJ*, 154, 28
- Bonatto, C., Bica, E., Ortolani, S., & Barbuy, B. 2007, *MNRAS*, 381, 45
- Borissova, J., Chené, A.-N., Ramírez Alegria, S., et al. 2014, *A&A*, 569, 24
- Cardelli, J. A., Clayton, G. C., & Mathis, J. S. 1989, *ApJ*, 345, 245
- Cohen, R., et al. 2017, *MNRAS*, 464, 1874
- Contreras Ramos, R., Zoccali, M., Gran, F., et al. 2017, *A&A*, in press (arXiv:1709.07919)
- Cote, P., Marzke, R. O., West, M. J., & Minniti, D. 2000, *ApJ*, 533, 869
- De Grijs, R., & Bono, G. 2017, *ApJS*, 227, 5
- Emerson, J., & Sutherland, W. 2010, *Msngr*, 139, 2
- Froeblich, D., Meusinger, H., & Scholz, A. 2008, *MNRAS*, 390, 1598
- Gonzalez, O. A., Rejkuba, M., Zoccali, M., et al. 2012, *A&A*, 543, 13
- Grocholski, A. J., & Sarajedini, A. 2002, *AJ*, 123, 1603
- Harris, W. E. 1996, *AJ*, 112, 1487
- Harris, W. E. 2010, arXiv:1012.3224
- Harris, W. E., et al. 2013, *ApJ*, 772, 82
- Helmi, A., & White, S. D. M. 1999, *MNRAS*, 307, 495
- Huxor, A. P., Mackey, A. D., Ferguson, A. M. N., et al. 2014, *MNRAS*, 442, 2165
- Ibata, R., Gilmore, G., & Irwin, M. 1994, *Natur*, 370, 194
- Ivanov, V. D., & Borissova, J. 2002, *A&A*, 390, 937
- Ivanov, V. D., Kurtev, R., & Borissova, J. 2005, *A&A*, 442, 195
- Ivanov, V. D., Piatti, A., Beamin, J. C., et al. 2017, *A&A*, 600, 112
- Kim, D., & Jerjen, H. 2015, *ApJ*, 799, 73
- Kim, D., Jerjen, H., Mackey, D., Da Costa, G. S., & Milone, A. P. 2016, *ApJ*, 799, 73
- Kim, D., et al. 2015, *ApJ*, 803, 63
- Koposov, S., de Jong, J. T. A., Belokurov, V., et al. 2007, *ApJ*, 669, 337
- Laevens, B. P. M., Martins, N., Sesar, B., et al. 2014, *ApJL*, 786, L3
- Longmore, A. J., Kurtev, R., Lucas, P. W., et al. 2011, *MNRAS*, 416, L465
- Majaess, D., Turner, D., & Gieren, W. 2011, *ApJL*, 741, L36
- Minniti, D. 1995, *AJ*, 109, 1663
- Minniti, D., Hempel, M., Toledo, I., et al. 2011, *A&A*, 527, L81
- Minniti, D., Lucas, P. W., Emerson, J. P., et al. 2010, *NewA*, 15, 433
- Minniti, D., Palma, T., Dekany, I., et al. 2017, *ApJL*, 838, L14
- Moni Bidin, C., Mauro, F. D., Geisler, D., et al. 2011, *A&A*, 535, 33
- Muñoz, R. R., Geha, M., Cote, P., et al. 2012, *ApJL*, 753, L15
- Ortolani, S., Bica, E., & Barbuy, B. 2006, *ApJL*, 646, L115
- Ortolani, S., Bonatto, C., Bica, E., & Barbuy, B. 2009, *AJ*, 138, 889
- Palma, T., Minniti, D., Dekany, I., Claria, J. J., & Alonso-Garcia, J. 2016, *NewA*, 49, 50
- Saito, R. K., Hempel, M., Minniti, D., et al. 2012, *A&A*, 537, A107
- Sakamoto, T., & Hasegawa, T. 2006, *ApJL*, 653, L29
- Schlafly, E. F., & Finkbeiner, D. P. 2011, *ApJ*, 737, 103
- Tissera, P., Machado, R. E. G., Carollo, D., et al. 2017, *MNRAS*, in press (arXiv:1709.0665)
- Valenti, E., Ferraro, F. R., & Origlia, L. 2004, *MNRAS*, 351, 1204
- Weinberg, M. D. 1994, *AJ*, 108, 1414
- York, D. G., Adelman, J., Anderson, J. E., Jr., et al. 2000, *AJ*, 120, 1579